Published in Thin Solid Films 515, issue 3, 952-956, 2006
which should be used for any reference to this work

Optical, electrical and mechanical properties of the tantalum oxynitride thin films deposited by pulsing reactive gas sputtering

H. Le Dréo [a,*], O. Banakh [a], H. Keppner [a], P.-A. Steinmann [a], D. Briand [b], N.F. de Rooij [b]

[a] *University of Applied Sciences, HE-ARC Ingénierie, Av. Hôtel-de-Ville, 7, CH-2400 Le Locle, Switzerland*
[b] *Institute of Microtechnology, University of Neuchatel, rue Jaquet-Droz 1, P.O. Box 526, CH-2002 Neuchâtel, Switzerland*

Abstract

Thin films of tantalum oxynitride were prepared by reactive magnetron sputtering using a Ta target and N_2 and O_2 as reactive gases. The nitrogen flow was kept constant while the oxygen flow was pulsed periodically. The film composition evolves progressively from $TaO_{0.25}N_{1.51}$ to $TaO_{2.42}N_{0.25}$ while increasing the oxygen pulse duty cycle without any abrupt change in the elemental content. The optical transmission spectra of the films deposited on glass show a "blue shift" of the absorption edge with increasing oxygen content. X-ray diffraction (XRD) patterns of all films exhibit broad peaks typical for nanocrystalline materials. Cross-section film morphology is rather featureless and surface topography is smooth exhibiting very small grains, in agreement with the results obtained by XRD. The optical properties of the films are very sensitive to their chemical composition. All films exhibit semiconducting behaviour with an optical band gap changing from 1.85 to 4.0 eV with increasing oxygen content. In order to evaluate the potential of the tantalum oxynitride films for microelectronic applications some Ta–O–N films were integrated in a MOS structure. The results of the capacitance–voltage measurements of the system Al//Ta–O–N//p-Si are discussed with respect to the chemical composition of the Ta–O–N films.

Keywords: Tantalum oxynitrides; Magnetron sputtering

1. Introduction

Modern materials science aims at the development of multifunctional materials designed for the applications in different industrial branches. This challenging task could be reached by the combination of many desirable properties in one material. Transition metal oxynitrides (TM–O–N) are considered as promising multifunctional materials. A variety of the potential applications anticipated for metal oxynitrides (electrochromic coatings, biocompatible coatings, nanocrystalline solar cells and catalysts, selective solar absorbers [1–4]) is a result of the wide range of chemical compositions of TM–O–N determining their physical, chemical and functional properties. The interest in transition metal oxynitrides progressively increases, and a considerable number of publications devoted to them appears in the scientific literature [5–8]. Recently, it was shown that TM–O–N (TM=Ti, Zr, Hf, Ta) films deposited by magnetron sputtering exhibit improved optical properties (high refractive index and transmittance in the visible, low roughness) compared to pure oxides [9]. It makes them attractive for microelectronic (gate dielectrics, diffusion barriers), optical applications (antireflection coatings), and as biocompatible coatings [10–14].

Previously we reported on the properties of the Ta–O–N thin films deposited by reactive magnetron sputtering with a simultaneous injection of two reactive gases (N_2 and O_2) [15]. It was shown that the incorporation of oxygen into the original nitride lattice leads to progressive structural and compositional changes, resulting in the variation of the optical and mechanical properties. However, this method suffers from plasma instabilities due to the non-linear relationship between the reactive gas flow rate and sputtering rate, resulting in a difficulty to control the chemical composition of the films [16]. This drawback can be overcome by using a reactive gas pulsed magnetron sputtering method. Nitrogen mass flow rate is maintained constant whereas that of oxygen is pulsed during the

* Corresponding author. Tel.: +41 32 930 14 70; fax: +41 32 930 29 30.
E-mail address: herve.ledreo@he-arc.ch (H. Le Dréo).

deposition allowing an easy adjustment of the non-metal content in the films. The details on this process were reported elsewhere [17]. The films reported in this study were produced by a reactive pulsing process but using different as in [17] process parameters and chamber geometry. The present paper is focused on the relationship between process parameters, chemical composition, optical, electrical, and mechanical properties of the sputtered Ta–O–N films.

2. Experimental details

The sputtering experiments were performed in an Alcatel A450 vacuum chamber evacuated by a pumping unit to the base pressure of 2×10^{-4} Pa. The pumping speed was 14 L/s. Ta–O–N films were deposited by direct current (DC) reactive magnetron sputtering from a metallic Ta target (99.96% purity, 100 mm diameter) using N_2 and O_2 as reactive gases. Depositions were carried out in a constant current mode (current density J = 0.01 A/cm^2). Prior to the film deposition, the target was sputter cleaned in an Ar plasma at a pressure of 0.5 Pa for 10 min. The substrates (Si wafer, microscopy glass) were ultrasonically cleaned in acetone (5 min) and isopropanol (5 min). Prior to film deposition, the substrates were sputtered in Ar plasma for 10 min by applying a negative bias voltage. During the deposition, the substrates were electrically grounded; no additional heating was applied to the substrates. The target-to-substrate distance was 89 mm. The N_2 supply was kept constant while the O_2 introduction was turned *on* and *off* by a flow-meter controlled valve. The cycle period ($T = t_{ON} + t_{OFF}$) was fixed at 40 s. The t_{ON} time of the oxygen pulse length was systematically changed from 4 to 32 s, resulting in the variation of the duty cycle, $\alpha[\%] = (100\times t_{ON})/T$, from 10 to 80%. The *on* and *off* oxygen flow rates (qO_{2max} and qO_{2min}) were adjusted at 6 and 0 sccm, respectively. The Ar partial pressure during deposition was kept constant at 0.5 Pa and the total pressure varied from 1.1 to 1.7 Pa. The deposition time was 15 min, resulting in a film thickness varying between 386 and 560 nm. Thicker coatings (3 μm) were deposited for mechanical tests.

The chemical composition of the films was determined by Rutherford backscattering spectroscopy (RBS). A 2 MeV He^+ beam and a 2 MeV proton beam were used. The analysed area was 0.5×0.5 mm^2. In addition, impurities like Ar were checked by particle induced X-ray emission (PIXE) using protons because of the increased sensitivity for traces or minor elements. The relative errors of RBS and PIXE are about 5 and 10%, respectively.

The cross-section morphology of the films on Si substrates was observed by scanning electron microscopy (SEM, JEOL JMS-6400F) at an acceleration voltage of 5 keV. The surface topography was analysed by atomic force microscopy (AFM, Nanoscope III, Digital Instruments) in contact mode on a sample area of 1 μm^2 with a scanning frequency of 1 μm/s. The structure of the films was studied by X-ray diffraction (XRD, Rigaku) at grazing incidence (4°) using a CuK_α radiation. The transmittance of the films deposited on glass substrates was measured as a function of wavelength (from 200 to 1100 nm) with a Perkin-Elmer spectrophotometer. The optical properties of the films were determined with a phase-modulated spectroscopic ellipsometer (UVISEL HR460, Jobin-Yvon Horiba Group) at an incidence angle of 70° in the energy range 0.75–4.50 eV. The optical band gap E_g was derived from the Tauc plot, $(\alpha h\nu)^{1/2}$ versus $h\nu$ and by extrapolating the straight line to the abscissa (α is the absorption coefficient, $h\nu$ the photon energy,), assuming an indirect transition occurring in Ta_2O_5 [18]. Hardness H and elastic modulus E of the coatings were measured by a nanoindentation depth-sensing technique (Nanohardness Tester, CSM Instruments SA) using a Berkovich-type diamond indenter. The maximum load (10 mN) was adjusted in order to insure a penetration depth of less than 10% of the coating thickness. The values of H and E were determined by using the method described by Oliver and Pharr [19].

In order to study the dielectric characteristics of the films, Al//Ta–O–N//Si metal-oxide-semiconductor (MOS) structures were fabricated and the film capacitance–voltage ($C–V$) characteristics were measured. Three films with chemical composition $TaO_{1.00}N_{1.09}$, $TaO_{1.96}N_{0.69}$ and $TaO_{2.32}$ were deposited on p-type (100), 100 mm in diameter, 525-μm-thick Si wafers. The film thickness over the wafer, exhibiting a gradient due to the inhomogeneity of the deposition, was between 80 and 150 nm. The film thickness was precisely determined by ellipsometry at each point where the capacitance measurement was performed. These values combined with the capacity (C_{ox}) of the dielectric films in the accumulation regime of the $C–V$ measurements were considered for the calculation of the permittivity, ε_s. Even with the presence of a gradient of thickness, the deviation of ε_s is lower than 10% for each film. The metallization was done by evaporation of 300 nm-thick Al dots through a shadow mask with an area of 0.78 cm^2 on the surface of the films. The $C–V$ characteristics of the MOS capacitor were measured using a HP 4275A Multifrequency LCR METER at 1 MHz. The temperature was kept constant at 299 K by a temperature controller. The details on the $C–V$ measurements can be found in [20]. To improve the quality of the MOS structures, a two-step post-metallization annealing (PMA) was performed. PMA is usually used in microelectronics in MOS capacitor fabrication in order to densify the Al dots and to reduce the number of charges present at the interfaces and in the film [21]. The first annealing step was executed in

Table 1
Chemical composition and thickness of the Ta–O–N films deposited at different duty cycles, α

α, %	Ta, at.%	N, at.%	O, at.%	N/Ta	O/Ta	(O+N)/Ta	Thickness, nm
10	35.7	54	8.9	1.51	0.25	1.76	551
20	34.4	46.5	18.3	1.35	0.53	1.88	538
30	33.3	41.7	23.9	1.25	0.72	1.97	552
40	32.1	35.1	32.2	1.09	1.00	2.10	564
50	29.8	28.5	40.9	0.96	1.37	2.33	558
60	27.2	18.8	53.2	0.69	1.96	2.65	507
80	27.1	6.9	65.5	0.25	2.42	2.67	386

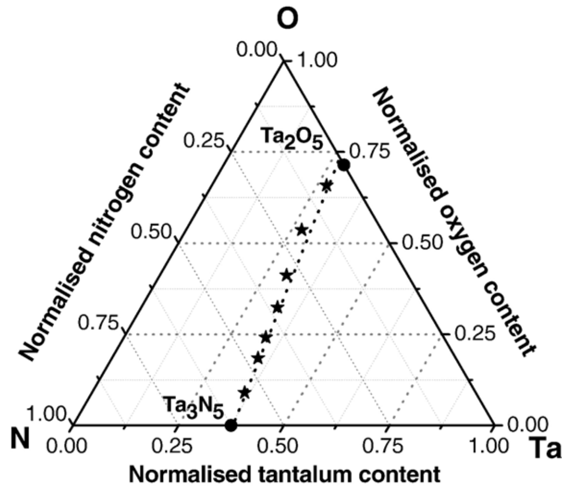

Fig. 1. Ternary Ta–O–N system representing the chemical composition of the deposited films (stars). The composition of Ta_2O_5 and Ta_3N_5 is shown for reference.

N_2 at 723 K for 30 min and the second one in forming gas (H_2:N_2 = 10:90, by volume) at 723 K for 30 min.

3. Results and discussion

3.1. Chemical composition, structure and morphology

Table 1 shows the chemical composition of the Ta–O–N films, the elemental content (in at.%), O/Ta, N/Ta and (O+N/Ta) ratios, as function of the duty cycle, α. As the oxygen concentration in the plasma increases with the duty cycle (longer oxygen pulse time, t_{ON}), its concentration in the films also progressively increases, while the nitrogen content decreases. The Ta content decreases from 35.7 to 27.1 at.%. Increasing α also results in the increase of the non-metal content in the films from 1.76 to 2.67. As it is seen from the ternary Ta–O–N diagram (Fig. 1), the chemical composition of the films spans the range between Ta_3N_5 and Ta_2O_5. A smooth evolution of the chemical composition from tantalum nitride to tantalum oxide suggests the progressive replacement of the nitrogen atoms by the oxygen ones in the lattice. However, it is rather impossible to realise such a replacement without important structural changes. We suppose that the tantalum oxynitrides are complex materials composed of several phases (TaN, Ta_3N_5, Ta_2O_5...), where a fraction of each phase depends of the actual composition of the film.

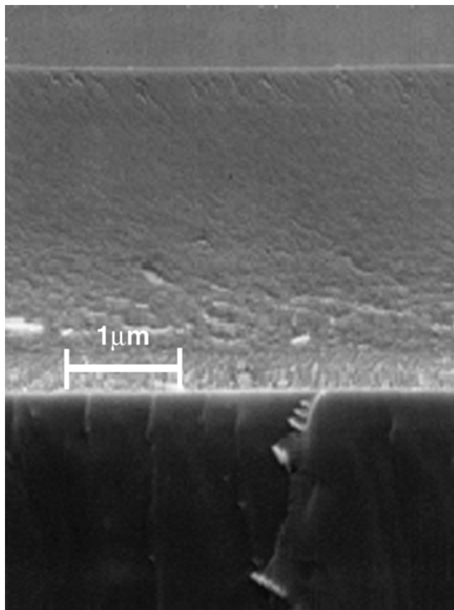

Fig. 2. Cross-section film morphology (SEM micrograph) of 3 µm-thick Ta–O–N film deposited on Si at the duty cycle of 50%.

XRD patterns of Ta–O–N films exhibit very broad peaks making phase identifications difficult. Such patterns are a signature of a disordered structure of the films and/or a very small crystallite size (a few nanometers). Taking into account the chemical composition of the films (namely their non-metal content) we suppose that with increasing non-metal content the structure develops from tetragonal Ta_3N_5-type for the $TaO_{0.25}N_{1.51}$ film to the tetragonal or orthorhombic Ta_2O_5-type for the $TaO_{2.46}N_{0.25}$ film, passing through some intermediate phases.

The SEM cross-section film morphology of the 3 µm-thick film deposited with α = 50% (Fig. 2a) shows a featureless structure, typical for the films with extremely fine grains, as observed by XRD. This morphology is similar for all studied films. The surface topography of all films, analysed by AFM, is smooth and the surface roughness is lower than 0.5 nm (comparable with the resolution of AFM). Again, this topography is typical for films with nanoscopic grains in agreement with XRD and SEM observations.

3.2. Optical properties

The optical transmittance at a wavelength of 633 nm of the Ta–O–N films deposited on glass increases from 8 to 84% with the non-metal content (Fig. 3), the coatings change their aspect from semi-absorbent (nitride-like) to transparent (oxide-like). In addition, the absorption edge shifts to higher energy values, indicating an increase of the optical band gap (E_g) from 1.85 to 4.0 eV, as measured by ellipsometry. The insulating behaviour of the Ta–O–N films becomes more pronounced with an increasing (O+N)/Ta ratio (and O content), and is a result of the incorporation of oxygen in the film. The mechanism of oxygen

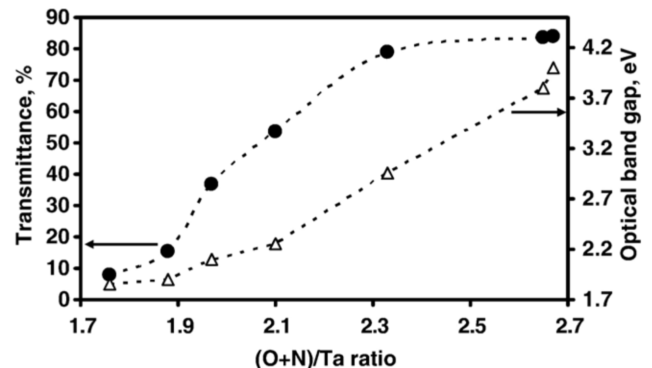

Fig. 3. Transmittance (taken at 633 nm) of the Ta–O–N films deposited on glass and optical band gap measured by spectroellipsometry.

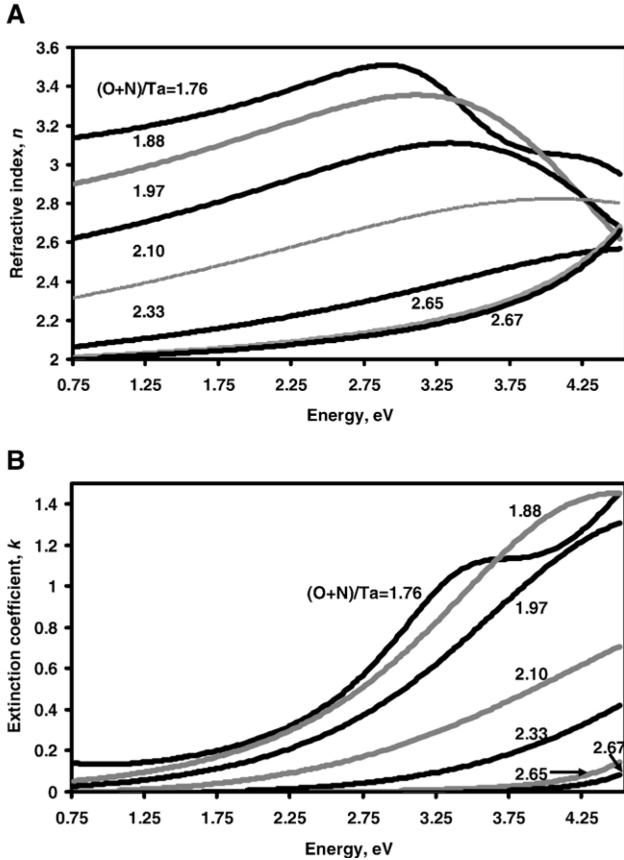

Fig. 4. Dispersion of refractive index (a) and extinction coefficient (b) of the Ta–O–N films with different metalloid content (O+N)/Ta.

incorporation in the film is not clear. One can suppose its incorporation into the lattice by a substitution of nitrogen atoms by oxygen ones, or an increase of the fraction of the insulating oxide phase, considering tantalum oxynitride as a composite material. In both cases the percentage of the ionic bonds in tantalum oxynitride increases, while the part of the covalent Ta–N bonds is diminished. Oxygen is more electronegative than nitrogen, therefore the electronic charge transfer from Ta towards O is higher than for Ta–N bonds, resulting in an increase of ionicity in Ta–O–N.

Refractive index *n* and extinction coefficient *k* of the films, as measured by spectroellipsometry, are presented in Fig. 4. The optical properties of the Ta–O–N films evolve progressively with the chemical composition. The (O+N)/Ta of 2.65 could be considered as a threshold value, above which the optical parameters (*n, k*) do not change and tend to that of stoichiometric Ta_2O_5 [22]. By contrast, the optical band gap E_g values continue to increase above this threshold due to an important change in the chemical composition.

3.3. Hardness and Young's modulus

Nanohardness *H* and Young's modulus *E* were measured for three 3 μm-thick Ta–O–N films deposited at the duty cycles $\alpha=10$, 30 and 50%. The hardness values are 14.0, 9.7 and 7.3 GPa, respectively, and the Young's modulus values are 233.2, 182.4 and 146.8 GPa, respectively. Both *H* and *E* values show a clear dependence on the chemical composition, decreasing with the non-metal content. A similar trend was observed for the Ta–O–N films deposited by conventional reactive magnetron sputtering [15] and other sputtered TM–O–N films [5]. It can be concluded that chemical composition is the key factor governing the mechanical properties of the oxynitride films. An increase of the non-metal content in the film leads to a lower fraction of the strong covalent TM–N bonds, which results in the decrease of *H* and *E* values.

3.4. Electrical properties

In order to study the dielectric characteristics of the Ta–O–N films, the Al//Ta–O–N//Si metal-oxide-semiconductor (MOS) structures were fabricated and the Ta–O–N film *C–V* characteristics were measured. Three films of chemical composition $TaO_{1.00}N_{1.09}$, $TaO_{1.96}N_{0.69}$ and $TaO_{2.32}$ were studied. The influence of the composition on the electrical properties of the as-deposited films was studied first. The *C–V* plot of the films (Fig. 5a) shows that the higher the O content in the film, the more the flat-band voltage (V_{fb}) shifts to 0 V. Average V_{fb} of $TaO_{1.00}N_{1.09}$ film is at −8.5 V, whereas that of $TaO_{2.32}$ film is at 0.14 V. Moreover, an increasing O content results in the reduction of the depletion zone. In conclusion, as-deposited Ta–O–N films seem to contain an important amount of charges, both in the film and at the interfaces with Al and Si. A

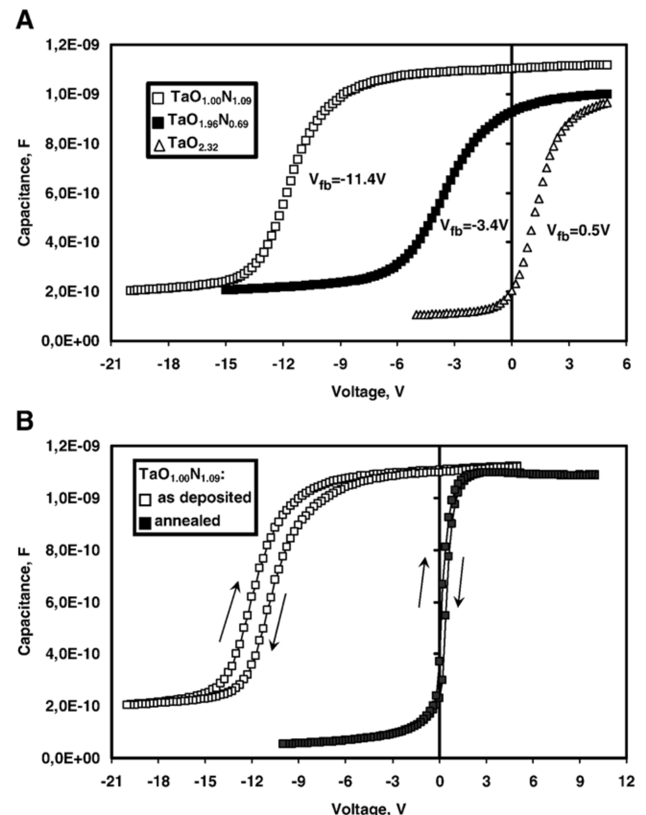

Fig. 5. (a) *C–V* curves of three as-deposited Ta–O–N films incorporated in MOS structures with actual values of V_{fb} (average V_{fb} values are reported in the text); (b) *C–V* curves of the as-deposited and annealed $TaO_{1.00}N_{1.09}$ film.

promising result is that permittivity (ε_s) increases with increasing N content. The value of ε_s for the $TaO_{2.32}$ film is 14, while for the $TaO_{1.00}N_{1.09}$ film its value reaches 23.

Thin films produced by sputtering may show a low density and also the presence of structural defects. Dislocations, interstitial atoms, vacancies, impurities, stacking faults are typical defects usually present in the film, while dangling bonds and nonbringing oxygen are located at the film–silicon interface. These defects result in a significant amount of the charges present in the oxynitride films and its interface with Si and it leads to the deterioration of the film electrical properties. In order to improve the film *C–V* characteristics, a two-step post-metallization annealing of the MOS structures was performed. The impact of the first annealing step is the most significant for the coating with the lowest O content, leading to the decrease of both the V_{fb} and the effective number of charges per unit area (N_{ss}, number/cm^2) in the film (Fig. 5b). The second annealing step only affects the N_{ss} of the $TaO_{1.00}N_{1.09}$ film by reducing it by 7 (from 8.0×10^{12} cm^{-2} for as-deposited film to 3.8×10^{12} cm^{-2} for the film after the first annealing step and to 5.0×10^{11} cm^{-2} after the second annealing step).The permittivity is only slightly affected, a decrease of ε_s (3–10%) upon annealing was observed for all the films.

In summary, the annealing process is necessary to improve the quality of the Ta–O–N films by reducing the number of charges both in the film and at the interfaces, and by shifting the V_{fb} value close to zero. In addition, the hysteresis is significantly reduced for all the films after annealing. A weak point of annealing is that the permittivity of the films slightly decreases. Taking into account the V_{fb} (lower than 1 V) and N_{ss} (less than 1.0×10^{12} cm^{-2}) of the annealed Ta–O–N films, they can be considered for applications in MOS devices.

4. Conclusions

Ta–O–N films were prepared by reactive magnetron sputtering using a pulsed flow of oxygen, while keeping the nitrogen flow constant. By modifying the main process parameter, duty cycle, the composition of the films evolves progressively, spanning the whole range between Ta_3N_5 and Ta_2O_5. Optical and mechanical properties of the films were studied with respect to their composition, namely the non-metal content. It was shown as the non-metal content in the films increases from 1.76 to 2.67, the films become more transparent (transmittance changes from 8 to 82%) and insulating (E_g varies from 1.85 to 4.0 eV). Optical parameters (*n, k*) both decrease with (O+N)/Ta and stabilize at $(O+N)/Ta\geq2.65$. Hardness and elastic modulus decrease with an increasing non-metal content, a typical feature for many TM–O–N films.

From an application point of view it is important that optical and mechanical properties as well as the composition of the films vary progressively with process parameters, without any abrupt change. It results in very precise control of the coating properties by the process and allows the deposition of a coating with the properties needed for a specific application. The Ta–O–N coatings with low non-metal content are of interest for optical applications, where the combination of very high refractive index (2.5–3.3), large optical band gap (2.0–2.3 eV) together with the smooth dense morphology and high hardness is required.

The study of dielectric characteristics of some annealed Ta–O–N films, incorporated into MOS structure, shows that these films can be considered for applications in MOS devices, taking into account the V_{fb} (lower than 1 V) and N_{ss} (less than 1.0×10^{12} cm^{-2}).

Acknowledgements

The authors wish to thank Dr. N. Martin (ENSMM, Besançon, France) for the SEM and AFM characterizations and Dr. F. Munnik (CAFI, Le Locle, Switzerland) for the RBS measurements. The authors gratefully acknowledge the financial support of the European Community through the project “HARDECOAT” no. NMP3-CT-2003-505948, co-financed by the State Secretariat for Education and Research, Switzerland, no. OFES :03.0285-1.

References

[1] I. Tsyganov, T, M.F. Maitz, E. Wieser, E. Richter, H. Reuther, Surf. Coat. Technol. 200 (2005) 1041.
[2] R. Mientus, R. Grötschel, K. Ellmer, Surf. Coat. Technol. 200 (2005) 341.
[3] M.A. Aegerter, Sol. Energy Mater. Sol. Cells 68 (2001) 401.
[4] W. Assmann, Th. Reichelt, T. Eisenhammer, H. Huber, A. Mahr, H. Schellinger, R. Wolgemuth, Nucl. Instrum. Methods Phys. Res., B 113 (1996) 303.
[5] F. Vaz, P. Cerqueira, L. Rebouta, S.M.C. Nascimento, E. Alves, Ph. Goudeau, J.P. Rivière, K. Pischow, J. De Rijk, Thin Solid Films 447–448 (2004) 449.
[6] E. Misra, Y. Wang, N.D. Theodore, T.L. Alford, Thin Solid Films 457 (2004) 338.
[7] J.-M. Chappé, N. Martin, J.F. Pierson, G. Terwagne, J. Lintymer, J. Gavoille, J. Takadoum, Appl. Surf. Sci. 225 (2004) 29.
[8] P. Carvalho, F. Vaz, L. Rebouta, S. Carvalho, L. Cunha, Ph. Goudeau, J.P. Rivière, E. Alves, A. Cavaleiro, Surf. Coat. Technol. 200 (2005) 748.
[9] S. Venkataraj, D. Severin, S.H. Mohamed, J. Ngaruiya, O. Kappertz, M. Wuttig, Thin Solid Films 502 (2006) 228.
[10] M. Takayama, A. Noya, T. Sase, A. Ohta, K. Sasaki, J. Vac. Sci. Technol., B 14 (2) (1996) 674.
[11] M. Stavrev, D. Fischer, A. Preuss, C. Wenzel, N. Mattern, Microelectron. Eng. 33 (1997) 269.
[12] M. Stavrev, D. Fischer, C. Wenzel, K. Drescher, N. Mattern, Thin Solid Films 307 (1997) 79.
[13] O. Atsushi, S. Kazutomi, C. Kiyoshi, US Patent US5560998 (1996).
[14] S. Masahiko, H. Kazuhiko, O. Atsushi, US Patent US5786078 (1998).
[15] O. Banakh, P.-A. Steinmann, L. Dumitrescu-Buforn, Thin Solid Films 513 (2006) 136.
[16] C. Rousselot, N. Martin, Surf. Coat. Technol. 142–144 (2001) 206.
[17] O. Banakh, T. Heulin, P.E. Schmid, H. Le Dréo, I. Tkalcec, F. Lévy, P.-A. Steinmann, J. Vac. Sci. Technol., A 24 (2006) 328.
[18] F.E. Ghodsi, F.Z. Tepehan, Sol. Energy Mater. Sol. Cells 59 (1999) 367.
[19] W.C. Oliver, G.M. Pharr, J. Mater. Res 7 (1992) 1564.
[20] D. Briand, G. Mondin, S. Jenny, P.D. van der Wal, S. Jeanneret, N.F. de Rooij, O. Banakh, H. Keppner, Thin Solid Films 493 (2005) 6.
[21] E.H. Nicollian, J.R. Brews, MOS (metal oxide semiconductor) physics and technology, Wiley, New York, 1982 Chap. 15.
[22] E. Franke, M. Schubert, C.L. Trimble, M.J. DeVries, J.A. Woollam, Thin Solid Films 388 (2001) 283.